PAPER • OPEN ACCESS

Aerodynamic and Structural Assessment of Floating Wind Turbine Rotor Under Varying Tilt Angle

To cite this article: H H Mian *et al* 2024 *J. Phys.: Conf. Ser.* **2767** 022053

View the article online for updates and enhancements.

Aerodynamic and Structural Assessment of Floating Wind Turbine Rotor Under Varying Tilt Angle

H H Mian[1], M S Siddiqui[1], N Franchina[2], O Kouaissah[2], G Wang[3] and T A Nygaard[4]

[1]Department of Mechanical Engineering and Technology Management, Norwegian University of Life Sciences, 1432, Ås, Norway

[2]Department of Engineering and Applied Sciences, Università degli Studi di Bergamo, Viale Marconi 5, 24044 Dalmine (BG), Italy

[3]School of Aeronautics, Northwestern Polytechnical University, Xi'an 710072, PR China

[4]Institute for Energy Technology (IFE), P.O. Box 40, NO-2027 Kjeller, Norway

E-mail: `haris.hameed.mian@nmbu.no`, `muhammad.salman.siddiqui@nmbu.no`, `nicoletta.franchina@unibg.it`, `otman.kouaissah@unibg.it`, `wanggang@nwpu.edu.cn`, `Tor.Anders.Nygaard@ife.no`

Abstract. Predicting the aerodynamic performance of floating offshore wind turbines (FOWTs) proves challenging due to platform motion induced by waves. The effect of wind and waves results in a six-degree-of-freedom motion of the platform, directly influencing turbine performance. Understanding the impact of specific degrees of freedom (DOF) motions on aerodynamics and structural response is crucial for effective wind turbine design. This research examines the impact of rotor tilt on both aerodynamic performance and structural response. The investigation employs computational fluid dynamics (CFD) analysis and mapping aerodynamic loads onto the finite element (FE) mesh for structural analysis. The study employs a comprehensive 3D simulation, utilizing the moving reference frame (MRF) method for the NREL 5 MW reference wind turbine CFD simulations. It explores different rotor tilt angles ($5°$, $10°$, $15°$, and $20°$) encountered by offshore structures during their operation and examines their impact on aerodynamic performance. Predicted aerodynamic loads were mapped onto the blade FE mesh using the radial basis function (RBF) interpolation technique and solved using the open-source FE solver CalculiX. The analysis shows that the turbine performance is relatively unaffected up to a tilt angle of $10°$. However, further increase in rotor tilt angle adversely impacts turbine performance, leading to notable reductions in thrust and power output. The fluid-structure coupled analysis provided insights into the deformations and stresses experienced by the turbine blade, indicating a notable increase in flap-wise displacement for larger tilt angles, while edge-wise displacement is not as significantly affected. The maximum stress location on the blade generally correlates well with actual observations.

1. Introduction

Wind power has experienced rapid growth and has become an essential form of renewable energy. In 2021, electricity production from wind sources witnessed a substantial increase of nearly 273 TWh, marking a 17% rise [1]. This growth surpassed the previous year's achievement by 55% and stands as the highest among all power generation technologies [2]. Floating offshore wind turbines (FOWT) offer several advantages over fixed offshore wind power. They could be installed in deep waters and access richer wind resources, enhancing their potential for

energy generation [3]. According to research conducted by the US National Renewable Energy Laboratory (NREL), it is projected that the cost of FOWT will decrease at a faster rate compared to fixed offshore wind turbines [4]. The flow dynamics surrounding a rotating wind turbine blade are naturally complex due to wind shear, turbulence, and gusts. In the case of a FOWT, the flow characteristics become even more complex compared to those of a fixed wind turbine. This is primarily because the platform undergoes both translational and rotational movements [5].

Many researchers have previously investigated the influence of rotor tilt on wind turbine performance. Kim *et al.* [6] studied blade-tower interaction in tilted horizontal axis wind turbines (HAWT) through numerical simulations, finding a notable impact on aerodynamic loading. They noted significant interaction at the blade root, influenced by yaw error and wind shear, with tower radius variations having a greater effect than clearance variations. Narayana *et al.* [7] investigated using simpler, passive controls like the tilt-up method in small-scale wind turbines. They observed that this system relies on wind rotor drag to tilt the rotor upward during high winds. Their findings underscored that changing the tilt angle can improve the aerodynamic performance of small-scale wind turbines. Wang *et al.* [8] investigated the aerodynamic performance of a wind turbine at various tilt angles using STAR-CCM+ CFD software. They explored angles from 0° to 12° under uniform wind speed and shear. Using sliding mesh for blade rotation, they analyzed thrust, power, lift, drag, tip vortices, and velocity profiles. Results showed optimal performance at 4° tilt, affecting the angle of attack and thus thrust and power. The study aimed to assess tilt angle's impact on fixed wind turbine aerodynamics. Santo *et al.* [9] studied the impact of a 5° tilt angle on a large HAWT within a sheared wind velocity atmospheric boundary layer (ABL). They found that the tilt angle increased tip deflections due to gravitational load while reducing axial force oscillation. This led to larger tip displacements at specific azimuth angles, impacting internal stresses in blade structures and mitigating moments exerted on the hub. Based on the literature review presented, numerous researchers have dedicated their attention to investigating the aerodynamic performance of wind turbine blades under the tilt effect. However, there is a relatively limited exploration of the impact of adverse tilting (that could be possible in a floating scenario) on the aerodynamic characteristics and elastic deformations of the turbine blades. Therefore, this paper addresses this research gap by focusing on two key aspects. The first aspect involves conducting CFD analysis on a FOWT, considering different tilt angles. The second aspect entails mapping the aerodynamic loads obtained from the CFD analysis onto a finite element (FE) turbine blade model. This mapping process quantifies the extent of structural deformation and stress levels experienced by the blade. The subsequent section provides a comprehensive overview of the methodologies employed in this study. Following a detailed discussion of the methods, the geometric details of the NREL 5 MW turbine blade are presented, including specifics regarding the CFD and FE meshes. The subsequent section focuses on research outcomes, discussing the impact of rotor tilt angle variation through CFD simulations and analyzing the structural response of the turbine blade. The final section concludes with a summary of key findings and outlines potential areas for future work.

2. Methodology

In the present work, the three-dimensional, unsteady Reynolds averaged Navier-Stokes equations, coupled with the k-ω SST turbulence model, were implemented using the STAR-CCM+ software package [10]. The primary methodologies employed are the MRF and radial basis function (RBF) interpolation methods. The internal rotating frames were modeled using the MRF approach within a stationary computational mesh and reference frame. The RBF interpolation method plays an important role in facilitating data transfer from the fluid surface to the FE model of the wind turbine blade, ensuring an accurate and reliable exchange of information between two domains.

2.1. MRF method

There are different techniques to account for turbine rotation [11], with the chosen approach being the Moving Reference Frame (MRF) method based on the steady-state approximation [12]. This method involves translating fluid motion into a rotating frame. Its computational efficiency is notable due to the steady-state solution, making it less costly than alternatives such as the Sliding Mesh Interface (SMI) [13]. In the context of an inertial reference frame (i) and a rotating reference frame (r), the relationship between absolute velocity $(\vec{u}_i)$ in the inertial frame, rotating velocity $(\vec{u}_r)$, and angular velocity (Ω) is defined as follows:

$$\vec{u}_i = \vec{u}_r + \Omega \times \vec{r} \tag{1}$$

This equation expresses the absolute velocity in the inertial frame as a combination of the rotating velocity and the contribution from angular velocity. The compressible Reynolds-Averaged Navier-Stokes (RANS) equations, considering the inertial frame, and the mass conservation and momentum equations are given by:

$$\nabla \cdot (\rho \vec{u}_i) = 0 \quad \text{(Mass Conservation)} \tag{2}$$

$$\nabla \cdot (\vec{u}_i \otimes \vec{u}_i) = -\nabla \left(\frac{p}{\rho} \right) + \nabla \cdot (\mu \nabla \vec{u}_i) \quad \text{(Momentum Equation)} \tag{3}$$

These equations express mass conservation and momentum balance in the inertial frame, accounting for pressure, density, and viscous effects. The momentum equation in the rotating frame is then extended to include the Coriolis force $(\Omega \times \vec{u}_r)$:

$$\nabla \cdot (\vec{u}_r \otimes \vec{u}_i) + \Omega \times \vec{u}_r = -\nabla \left(\frac{p}{\rho} \right) + \nabla \cdot (\mu \nabla \vec{u}_i) \tag{4}$$

This equation introduces the Coriolis force resulting from the rotation of the reference frame into the balance of pressure, viscous forces, and turbulence effects influencing the absolute velocity. The variables ρ, μ, and p represent density, dynamic viscosity, and pressure, respectively.

2.2. RBF interpolation method

An enhanced point selection method employing RBFs was previously developed and validated [14, 15]. The method, rooted in a multi-level subspace RBF interpolation approach utilizing the 'double-edge' greedy algorithm, was developed to address the limitations of inaccurate interpolation inherent in single-point position correction processes. Through this approach, the method facilitates precise and high-quality data interpolation while minimizing computational costs. The expression for the necessary interpolation utilizing RBFs can be represented as:

$$F(\mathbf{r}) = \sum_{i=1}^{N} \phi_i(\|\mathbf{r} - \mathbf{r}_i\|) \cdot w_i \tag{5}$$

The expression $F(\mathbf{r})$ signifies the interpolated function at the point $\mathbf{r}$. Here, ϕ_i refers to the RBF associated with the i-th control point, and $\mathbf{r}_i$ represents the coordinates of this control point. The term $\|\mathbf{r} - \mathbf{r}_i\|$ denotes the Euclidean distance between the point of interest $(\mathbf{r})$ and the i-th control point. Additionally, w_i corresponds to the weights or coefficients assigned to each control point in the interpolation process. For a more comprehensive understanding and thorough validation of the method, readers are encouraged to refer to the work by Wang *et al.* [14]. The interpolation problem is described in the following universal form:
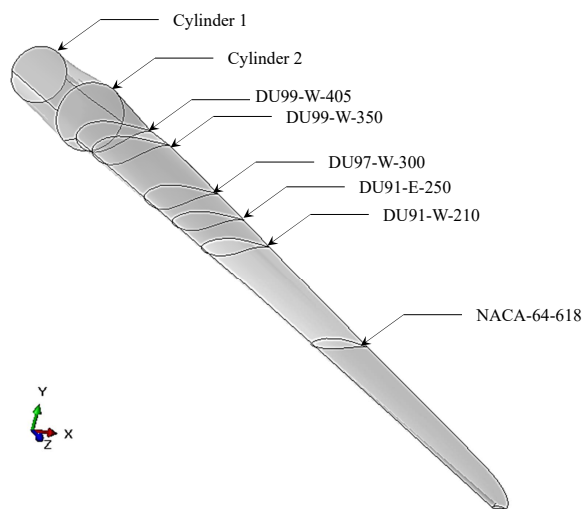
$$\Delta S = \phi W \tag{6}$$

Figure 1. NREL 5 MW: The turbine geometry is created with eight different sections blended to create the complete turbine blade.

Position(m)	Twist(deg)	Chord (m)	Section
0.00E+00	1.33E+01	3.386	Cylinder 1
1.37E+00	1.33E+01	3.386	
4.10E+00	1.33E+01	3.854	
6.83E+00	1.33E+01	4.167	Cylinder 2
1.03E+01	1.33E+01	4.557	DU99-W-405
1.44E+01	1.15E+01	4.652	DU99-W-350
1.85E+01	1.02E+01	4.458	
2.26E+01	9.01E+00	4.249	DU97-W-300
2.67E+01	7.80E+00	4.007	DU91-W-250
3.08E+01	6.54E+00	3.748	
3.49E+01	5.36E+00	3.502	DU93-W-210
3.90E+01	4.19E+00	3.256	
4.31E+01	3.13E+00	3.010	NACA-64-618
4.72E+01	2.32E+00	2.764	
5.13E+01	1.53E+00	2.518	
5.47E+01	8.63E+01	2.313	
5.74E+01	3.70E+01	2.086	
6.01E+01	1.06E+01	1.419	
6.15E+01	0.00E+00	1.085	

Table 1. Blade parameters (section position, twist angle, chord length, and section profile) for the NREL 5 MW reference wind turbine [16].

3. Geometry and computational meshes

3.1. Turbine geometry and specifications

The NREL 5 MW turbine blade [17, 18] is designed to produce the necessary power output under typical wind conditions. Figure 1 shows the geometry of the reference wind turbine, which comprises eight different section profiles combined to generate the complete blade geometry. The geometric details for the NREL 5 MW wind turbine blade are given in Table 1. The rotor has a diameter of 126 m, a hub diameter of 3 m, and a hub height reaching 90 m above ground level. This turbine exhibits a cut-in wind speed of 3 m/s, ensuring early energy capture, while the rated wind speed stands at 11.4 m/s, maximizing power generation. The cut-out wind speed is set at 25 m/s to ensure safe operation. Additionally, the turbine's rated rotor speed is specified at 12.1 rpm.

3.2. CFD mesh and boundary conditions

All the CFD simulations in the present work have been performed using the Star CCM+ solver [19]. There are several possible models for mesh generation within the solver. A trimmed cell model was employed to generate volume mesh. Different mesh and domain sizes have been tested to make the results independent of these parameters. Figure 2(a) shows the complete computational domain, with a size of eight million cells, generated for the NREL 5 MW wind turbine with specified velocity inlet and pressure outlet boundary conditions. The section cut of the domain is Figure 2(b), showing a dense region defined to capture the turbine's wake. Figure 2(c) shows the surface mesh for the turbine blades with blade refinement patches defined using the surface remesher option.

3.3. FE mesh of the blade

The turbine blade's FE model is generated and solved using an open-source FE solver, CalculiX [20]. The numerical model and the FE mesh are shown in Figure 3(a) and (b), respectively. The turbine blade is divided into 18 sections, and the material properties of each
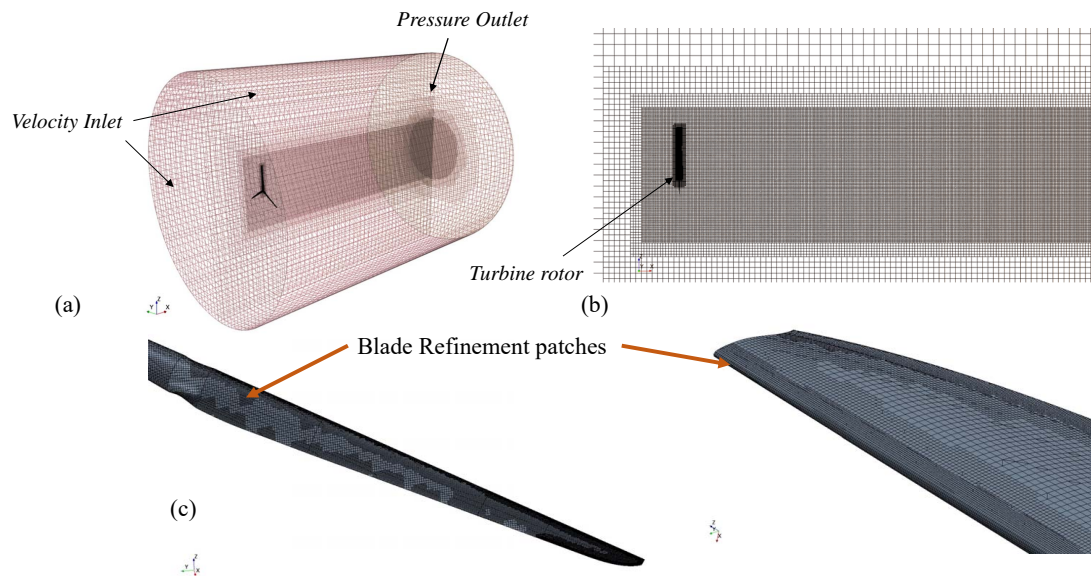
Figure 2. (a) CFD mesh of the NREL 5 MW showing complete fluid domain (b) Section cut to show the mesh refinement region for the wakes (c) Blade surface mesh with defined refinement patches at the leading edge curvatures.
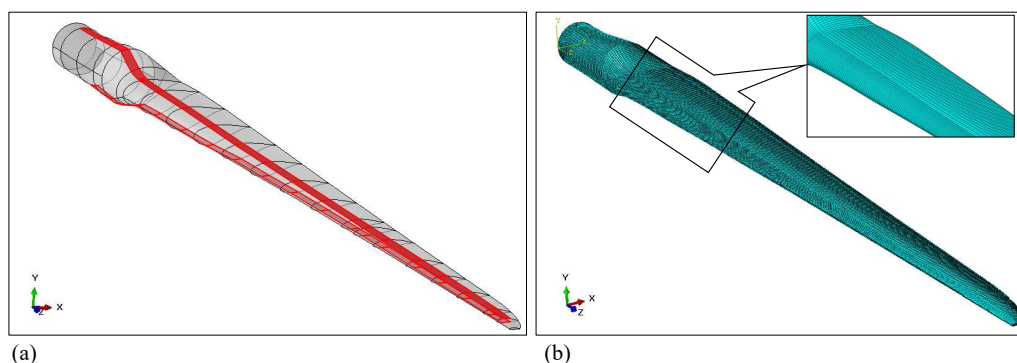

Figure 3. Numerical model of wind turbine blade structure for NREL 5 MW (a) Surface area with highlighted shear web defined at the center of the turbine blade (b) FE mesh generated for the turbine blade

section are defined. The materials employed include Gelcoat, unidirectional fibers, and foam. These materials, specific properties, and details have been adopted from the reference [17]. The FE model resulted in 28560 elements. The blade is fixed at the root, and the pressure data is mapped from the CFD mesh to the FE mesh using the RBF interpolation method. Figure 4 shows the variation of the FE model by comparing the total displacement of the turbine blade with the reference numerical model [21]. The maximum total displacement achieved in the current FE simulation is 2.503 m, in contrast to the reference total displacement of 2.596 m, which compares fairly well, indicating that the model is acceptable for subsequent analyses. Furthermore, Table 2 compares the modal frequencies of the blade obtained from CalculiX with reference values [17]. The modes include flapwise and edgewise bending as well as torsion. The results agree with a maximum percentage difference of 7.7% for mode 1.
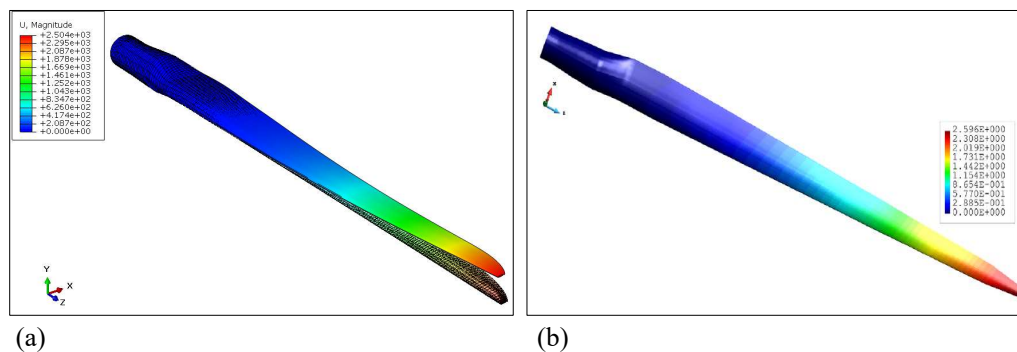
(a)   (b)

Figure 4. Comparison of the total displacement for the NREL 5 MW wind turbine blade (a) Present study (b) Reference FE results [21]

Mode	CalculiX	Ref [[17]]	Percentage Difference (%)	Description
1	0.803	0.87	7.701	1st flapwise bending
2	1.111	1.06	4.811	1st edgewise bending
3	2.535	2.68	5.410	2nd flapwise bending
4	3.945	3.94	0.127	2nd edgewise bending
5	5.602	5.57	0.575	3rd flapwise bending
6	6.125	6.45	5.039	1st torsion

Table 2. Comparison of CalculiX results with reference data and percentage differences

4. Results and discussion

4.1. Rotor tilt angle variation

To investigate the rotor tilt angle variation for the NREL 5 MW wind turbine blade, the initial analysis was conducted at a tilt angle of 0°. This study considered additional parameters, including a rated wind speed of 11.4 m/s and a rotor speed of 12.1 rpm, aligning with the NREL conditions [22] and used by several studies in literature [23, 24, 25]. This will facilitate the validation of the case setup, ensuring its suitability for subsequent analyses. The turbine rotations were specified through the implementation of the MRF method.

Different rotor tilt angles (0°, 5°, 10°, 15°, and 20°) have been simulated, and the turbine performance has been evaluated for comparison. Figure 5 (a) and (b) show the velocity contours and the vorticity magnitude, respectively, for different tilt angles. The rotor's tilt angle affects the blade's aerodynamic performance and, consequently, its interaction with the surrounding fluid. Figure 5 (c) compared the vorticity contours at 0° and 15° tilt angles. For a large tilt angle, the turbine blade rotates in the wake of the other blade affecting the aerodynamic characteristics of the rotor and leading to conditions such as wake interference, blade-blade interactions, and increased turbulence. Figure 6 shows the turbine performance plots for thrust, torque, and power produced for different rotor tilt angles. The results suggest that the turbine performance remains relatively stable up to a tilt angle of 10°. However, beyond this point, there is a notable degradation in performance. The rotor tilt angle also plays a critical role in influencing the distribution of loads on the turbine structure. Figure 7 compares the velocity profiles extracted from the near vicinity of the rotor at seven different sections (shown in Figure 7 (e)). 'Section 0' is just upstream of the turbine, while subsequent sections are positioned within the wake of the rotor blade, allowing for the observation of velocity deficit and turbulent flow effects. It can be seen from the figure that the velocity profile remains stable for tilt angles 0° and 5°, but some irregularity starts from a tilt angle of 10° which becomes more pronounced
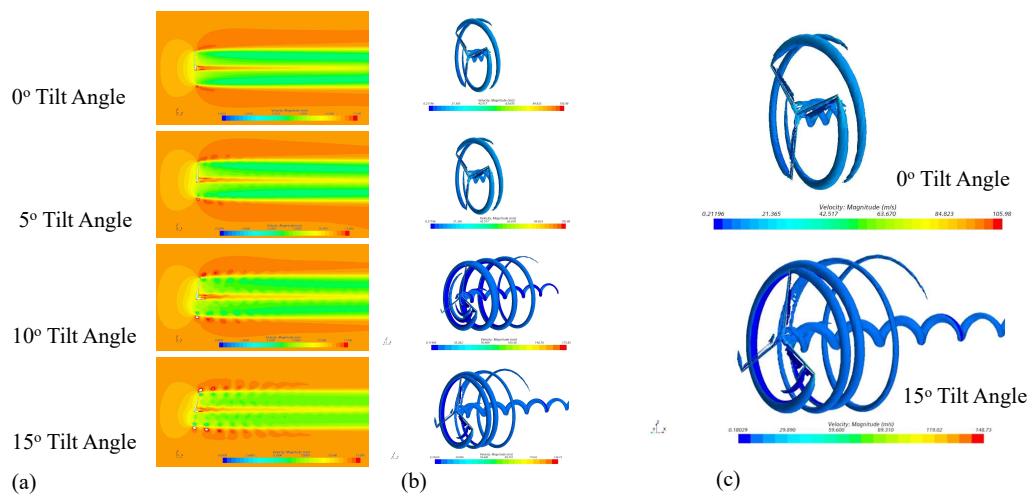
Figure 5. (a - b) Velocity and the vorticity magnitude for different rotor tilt angles (c) Comparison of the vorticity field at tilt angles of 0° and 15°, highlighting the impact of rotor tilt angle variation on the aerodynamic characteristics of the wind turbine blade
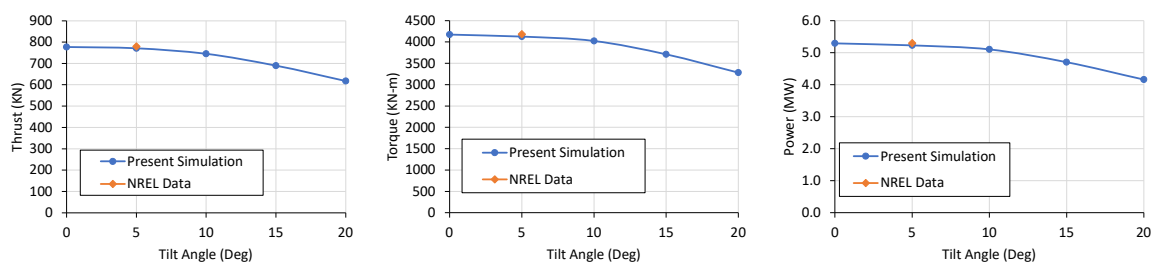

Figure 6. Performance plots for NREL 5 MW turbine, illustrating thrust, torque, and power variation across various rotor tilt angles.

for higher tilt angles. Furthermore, there is a noticeable disturbance in the velocity profile of the upstream section at higher tilt angles. These observations suggest potential performance degradation at higher tilt angles.

4.2. Fluid structure interaction analysis

The impact of varying rotor tilt angles on the turbine structure is investigated through a fluid-structure interaction (FSI) analysis. The approach employed in this study involves a one-way FSI analysis using the partitioned coupling approach. While a two-way interaction is feasible, a one-way interaction is selected to manage computational costs effectively. The pressure distribution estimated from the CFD analysis is mapped on the FE mesh of the turbine blade (shown in Figure 8 (b)). Due to the applied load, the turbine blade experiences structural deformation. Figure 9 (a) and (b) show the plots for the flap-wise and edge-wise displacement of the turbine blade, respectively. The structural response was determined by varying the tilt angle of the rotor. The results indicate that for rotor tilt angles of 0° and 5°, neither the flap-wise displacement nor the edge-wise displacement is significantly affected. However, there was a significant increase in flap-wise displacement for larger tilt angles (10°, 15°, 20°). The total flap-wise displacement nearly doubled with the tilt angle increasing from 5° to 20°. Although the edge-wise displacement also increased, the magnitude of this increase was not as pronounced as the flap-wise displacement.
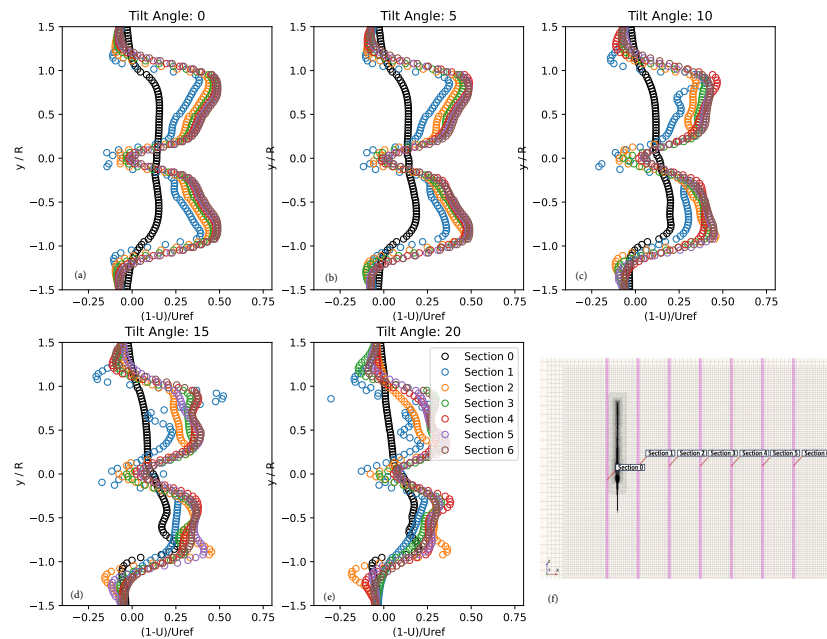
Figure 7. Velocity profile for at various locations, one upstream and several downstream of the rotor blade. (a - e) For different rotor tilt angles (f) data extraction lines showing different locations
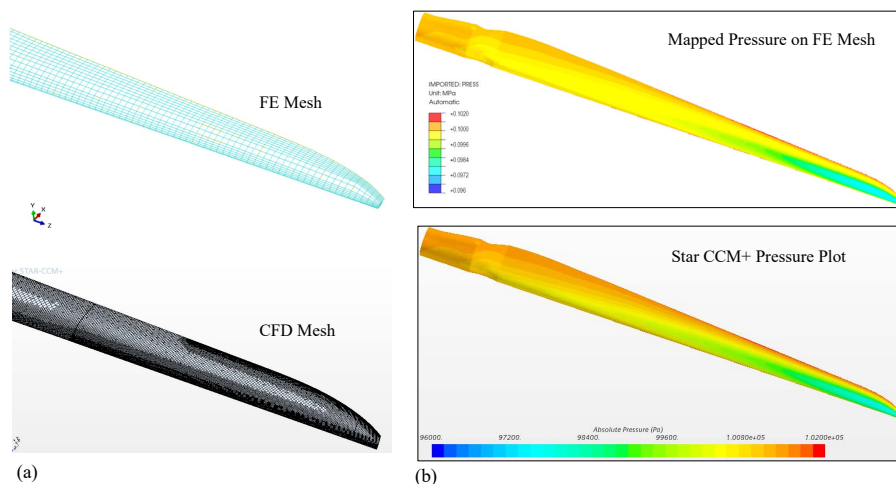

Figure 8. NREL 5 MW: (a) Comparing the CFD and FE mesh to compare the mesh density of the two models (b) Mapped pressure values from CFD to FE surface mesh

The equivalent stress estimated from this analysis is presented in Figure 10 (a) and (b) for two different tilt angles, 5° and 20°, respectively. It's essential to note that the analysis is static, and as such, the results may not entirely depict the true stress distribution that could be observed in a dynamic analysis. Despite this limitation, the equivalent stress contours provide valuable insights into the location of maximum stress. The identified location aligns with the typical scenario of blade structure failure, often occurring at approximately 35% to 40% of the span when measured from the blade's root. This correlation enhances the significance of the static analysis in identifying critical stress points in the turbine blade structure.
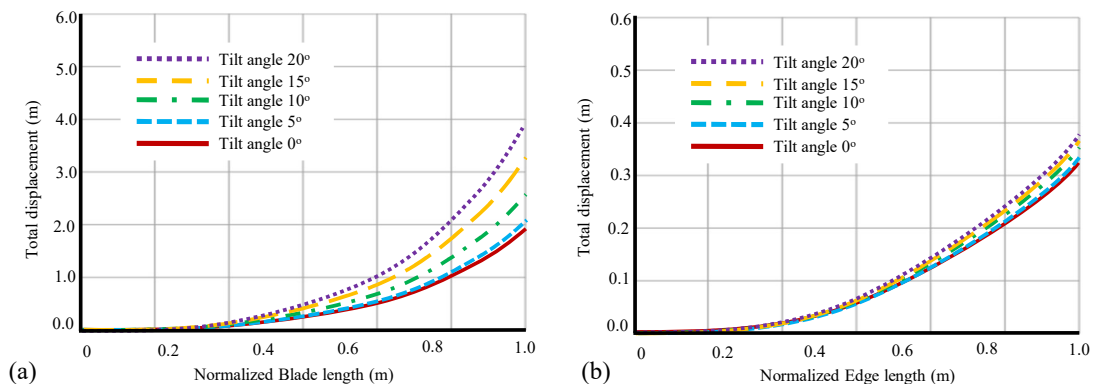
Figure 9. Total displacement plot at different rotor tilt angles (a) Flap-wise displacement (b) Edge-wise displacement
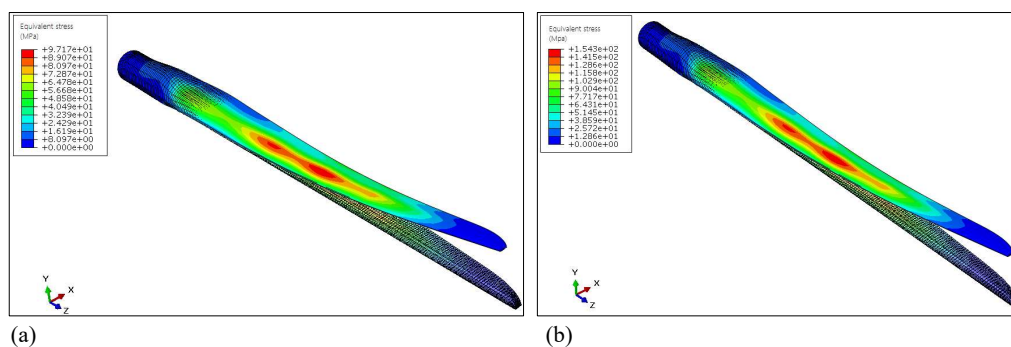

Figure 10. Equivalent stress plot for the wind turbine blade for different rotor tilt angles (a) 5° (b) 20°

5. Conclusion and future work

The research employed computational methods to analyze the impact of rotor tilt angle variation on both aerodynamic performance and structural response of the NREL 5 MW wind turbine blade. The FE model was validated against reference results found in the literature to ensure its suitability for subsequent analyses. Through CFD simulations, the study found that the turbine's performance remains stable up to a tilt angle of 10°, beyond which there is a degradation in the performance. The study also identified the intricate interplay between aerodynamic performance and structural response. The fluid-structure coupled analysis provided insights into the deformations and stresses experienced by the turbine blade, indicating a notable increase in flap-wise displacement for larger rotor tilt angles. In contrast, the edge-wise displacement is not as significantly affected. Despite the static nature of the stress analysis, the identified location of maximum stress correlated well with typical blade structure failure scenarios, enhancing the credibility of the numerical method. For future work, exploring dynamic FSI analyses could offer a more comprehensive understanding of the turbine's behavior under varying tilt angles. Investigating additional design parameters, such as blade material properties and structural configurations, could present results close to actual behavior.

References

[1] Global Wind Energy Council GWEC. Global wind report 2022, 2022.

[2] International Energy Agency IEA. Wind electricity, IEA, Paris, 2022.

[3] Bowen Zhou, Zhibo Zhang, Guangdi Li, Dongsheng Yang, and Matilde Santos. Review of key technologies for offshore floating wind power generation. *Energies*, 16(2):710, 2023.

[4] Ahmed I Osman, Lin Chen, Mingyu Yang, Goodluck Msigwa, Mohamed Farghali, Samer Fawzy, David W Rooney, and Pow-Seng Yap. Cost, environmental impact, and resilience of renewable energy under a changing climate: a review. *Environmental Chemistry Letters*, 21(2):741–764, 2023.

[5] Xinbao Wang, Chang Cai, Shang-Gui Cai, Tengyuan Wang, Zekun Wang, Juanjuan Song, Xiaomin Rong, et al. A review of aerodynamic and wake characteristics of floating offshore wind turbines. *Renewable and Sustainable Energy Reviews*, 175:113144, 2023.

[6] Hogeon Kim, Seungmin Lee, and Soogab Lee. Influence of blade-tower interaction in upwind-type horizontal axis wind turbines on aerodynamics. *Journal of Mechanical Science and Technology*, 25:1351–1360, 2011.

[7] Mahinsasa Narayana. Gyroscopic effect of small scale tilt up horizontal axis wind turbine. In *World Renewable Energy Congress VI Brighton, UK*, volume 1, 2000.

[8] Qiang Wang, Kangping Liao, and Qingwei Ma. The influence of tilt angle on the aerodynamic performance of a wind turbine. *applied sciences*, 10(15):5380, 2020.

[9] Gilberto Santo, Mathijs Peeters, Wim Van Paepegem, and Joris Degroote. Effect of rotor-tower interaction, tilt angle, and yaw misalignment on the aeroelasticity of a large horizontal axis wind turbine with composite blades. *Wind Energy*, 23(7):1578–1595, 2020.

[10] PLM Siemens. Simcenter STAR-CCM. *Academic Research, Release*, 12, 2017.

[11] David Hartwanger and Andrej Horvat. 3d modelling of a wind turbine using CFD. In *NAFEMS Conference, United Kingdom*, 2008.

[12] Thanhtoan Tran, Donghyun Kim, and Jinseop Song. Computational fluid dynamic analysis of a floating offshore wind turbine experiencing platform pitching motion. *Energies*, 7(8):5011–5026, 2014.

[13] Kobra Gharali and David A Johnson. Numerical modeling of an s809 airfoil under dynamic stall, erosion and high reduced frequencies. *Applied Energy*, 93:45–52, 2012.

[14] Gang Wang, Haris Hameed Mian, Zheng-Yin Ye, and Jen-Der Lee. Improved point selection method for hybrid-unstructured mesh deformation using radial basis functions. *Aiaa Journal*, 53(4):1016–1025, 2015.

[15] Haris Hameed Mian, Gang Wang, and Zheng-Yin Ye. Numerical investigation of structural geometric nonlinearity effect in high-aspect-ratio wing using CFD/CSD coupled approach. *Journal of Fluids and Structures*, 49:186–201, 2014.

[16] M Salman Siddiqui, Adil Rasheed, Mandar Tabib, and Trond Kvamsdal. Numerical investigation of modeling frameworks and geometric approximations on NREL 5 MW wind turbine. *Renewable Energy*, 132:1058–1075, 2019.

[17] Brian Ray Resor. Definition of a 5 MW/61.5 m wind turbine blade reference model. Technical report, Sandia National Lab (SNL-NM), Albuquerque, NM (United States), 2013.

[18] M Salman Siddiqui, Adil Rasheed, Mandar Tabib, and Trond Kvamsdal. Numerical analysis of nrel 5 MW wind turbine: A study towards a better understanding of wake characteristic and torque generation mechanism. In *Journal of Physics: Conference Series*, volume 753, page 032059. IOP Publishing, 2016.

[19] S Cd-Adapco. STAR CCM+ user guide version 12.04. *CD-Adapco: New York, NY, USA*, 62, 2017.

[20] Guido Dhondt. Calculix user's manual version 2.12. *Munich, Germany, accessed Sept*, 21:2017, 2017.

[21] Mingyang Li, Yildirim Dirik, Erkan Oterkus, and Selda Oterkus. Shape sensing of nrel 5 MW offshore wind turbine blade using iFEM methodology. *Ocean Engineering*, 273:114036, 2023.

[22] Jason Jonkman, Sandy Butterfield, Walter Musial, and George Scott. Definition of a 5 MW reference wind turbine for offshore system development. Technical report, National Renewable Energy Lab (NREL), Golden, CO (United States), 2009.

[23] Mandar Tabib, M Salman Siddiqui, Eivind Fonn, Adil Rasheed, and Trond Kvamsdal. Near wake region of an industrial scale wind turbine: comparing LES-ALM with LES-SMI simulations using data mining (POD). In *Journal of Physics: Conference Series*, volume 854, page 012044. IOP Publishing, 2017.

[24] Mandar Tabib, M Salman Siddiqui, Adil Rasheed, and Trond Kvamsdal. Industrial scale turbine and associated wake development-comparison of RANS based actuator line vs sliding mesh interface vs multiple reference frame method. *Energy Procedia*, 137:487–496, 2017.

[25] M Salman Siddiqui, Adil Rasheed, Trond Kvamsdal, and Mandar Tabib. Quasi-static & dynamic numerical modeling of full scale NREL 5 MW wind turbine. *Energy Procedia*, 137:460–467, 2017.